International Journal of Mechanical, Industrial and Aerospace Sciences
ISSN: 2517-9950
Vol:12, No:8, 2018

# Molding Properties of Cobalt-Chrome-Based Feedstocks Used in Low-Pressure Powder Injection Molding

Ehsan Gholami, Vincent Demers

***Abstract*—**Low-pressure powder injection molding is an emerging technology for cost-effectively producing complex shape metallic parts with the proper dimensional tolerances, either in high or in low production volumes. In this study, the molding properties of cobalt-chrome-based feedstocks were evaluated for use in a low-pressure powder injection molding process. The rheological properties of feedstock formulations were obtained by mixing metallic powder with a proprietary wax-based binder system. Rheological parameters such as reference viscosity, shear rate sensitivity index, and activation energy for viscous flow, were extracted from the viscosity profiles and introduced into the Weir model to calculate the moldability index. Feedstocks were experimentally injected into a spiral mold cavity to validate the injection performance calculated with the model.

***Keywords*—**Binder, feedstock, moldability, powder injection molding, viscosity.

## I. Introduction

RECENT developments in low-pressure powder injection molding (LPIM) can be attributed to the impressive growth rate of the conventional powder injection molding (PIM) technology, as well as the new requirements brought in by the automotive, medical, and aerospace sectors [1]-[5]. This manufacturing process consists of mixing metallic or ceramic powder with molten polymeric binder to obtain a feedstock with a powder solid loading typically ranging from 50 to 70 vol.%. The latter is then injected into a mold cavity to produce parts that are debound and sintered to completely remove the binder and obtain near-net shape dense metallic components [6], [7]. Over the last 15 years, low viscosity feedstocks formulated with low molecular weight polymers have been used in LPIM to increase moldability and shape complexity. A decrease in feedstock viscosity results in higher moldability at a lower pressure, thus minimizing the deformations of the mold, reducing tooling costs, and producing a laminar filling of the mold to promote defect-free parts.

Feedstock viscosity is one of the most important parameters influencing the success of the molding stage. The main variables influencing the feedstock viscosity are shear rate, temperature, solid loading, powder characteristics, and binder composition [8], [9]. Recent studies have demonstrated that feedstocks with a viscosity as low as 10 Pa·s can be used in the LPIM process [10], [11]. It has also been reported that the moldability index model developed for plastic injection molding [12], and more recently used in conventional metal injection molding [13]-[16] or in the LPIM of metal matrix composite parts [17], [18], could be used to predict the flow behavior of the feedstocks during injection. Although this moldability index has been used by several research teams, the experimental validation of this simple approach has received very little attention in the literature [19]. In addition, for Co-Cr-based feedstocks, the characterization of rheological behavior is still in its infancy, and the moldability index model has never been used to calculate the molding potential of such feedstocks. This work therefore aims to compare moldability index results with real scale injection results obtained with Co-Cr feedstocks used in LPIM.

E. Gholami is with the École de technologie supérieure, Montreal, QC, H3C 1K3, Canada.

V. Demers is with the École de technologie supérieure, Montreal, QC, H3C 1K3, Canada (corresponding author, phone: 514-396-8590; fax: 514-396-8530; e-mail: vincent.demers@etsmtl.ca).

## II. Experimental Procedures

### A. Material

Two gas-atomized cobalt-chrome (Co-Cr) powder lots with a spherical shape (Fig. 1) were used to produce two different feedstocks from a proprietary binder formulation. This Co-Cr alloy is widely used in aerospace, dentistry, and biomedical industries for its combination of high strength and relatively low density, leading to high specific strength properties, and its high wear resistance and excellent biocompatibility with blood and soft tissue, particularly for artificial knee, hip joint, coronary stent, and other surgical implants [20].

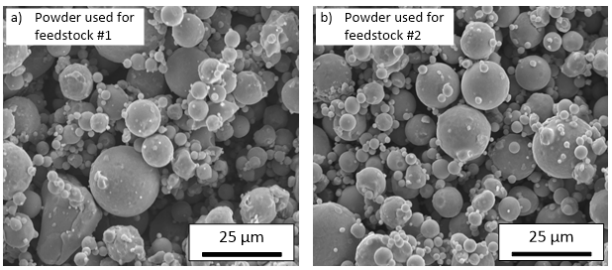


Fig. 1 SEM micrograph of the Co-Cr powder lots used to formulate feedstocks

### B. Characterization Methods

A scanning electron microscope (Hitachi 3600, SE detector) was used to qualitatively evaluate the particle characteristics

(shape, size, texture, agglomerate, etc.) of each dry powder lot. The viscosity profiles of each feedstock were obtained with an Anton Paar MCR 302 rotational rheometer using the CC-17 concentric-cylinder and the C-PTD 200 Peltier temperature-controlled measuring system. The rheological behavior of each feedstock was obtained at 70, 80, and 90 °C (i.e., above the melting point of feedstocks) over shear rates ranging from 0.5 to 400 $s^{-1}$. The feedstock, the cylinder, and the container were all pre-heated to the test temperature in order to reduce the thermal stabilization time and minimize the segregation of powder and binder that may occur during the rheological tests. Each testing condition was repeated twice with different samples.

Differential scanning calorimetry analysis (DSC) was performed with a PerkinElmer Pyris 1 to characterize the solid-liquid transitions and obtain the melting points of feedstocks. DSC specimens (mass ~ 15 mg) were encapsulated in standard aluminum hermetic pans using a universal crimper press and then tested over a 20 to 120 °C temperature range at a heating rate of 10 °C/min and under a nitrogen gas flow rate of 50 ml/min. Four DSC thermograms were performed (i.e., two heating and two cooling cycles), but only the second heating cycles were recorded in order to erase the previous thermal history and to maximize the thermal contact between the pan and specimen (c.f. ASTM D3418). Multiple DSC peaks exhibit several melting points associated with different binders in feedstock. In this project, the maximum mold temperature was set using the first peak obtained at lower temperatures on DSC thermograms (i.e., as indicated by a white arrow in Fig. 3 (a)), while the feedstock melting point was determined from the last peak obtained at higher temperatures on the DSC curves (i.e., as indicated by a black arrow in Fig. 3 (a)). The latter value corresponds to the minimum temperature required to completely melt the feedstock before the injection and rheology tests, as recommended in [21].

A laboratory injection press (Fig. 2 (a)) was used for injecting feedstocks into a spiral mold (Fig. 2 (b)), which was designed to minimize the segregation of low viscosity feedstocks using a new injection concept [22]. This injection system consists in eliminating the interconnecting pipe and injection valve by using a sliding platform concept, which was adapted for the transportation of the feedstock from the container to the mold cavity. During an injection sequence, the injection system withdraws the desired volume of feedstock from the feedstock container, which is then aligned with the gate of the mold by displacing the sliding table to move the injection system (i.e., the injection table is slid with respect to the feedstock container, the latter being maintained by the mixing system). Since the container outlet can be closed off without the need for an injection valve, the segregation of feedstock inside the valve is avoided, maintenance of the closing mechanism is limited, cleaning is simplified, and contamination of the feedstock is minimized. The feedstock is then injected into the mold cavity, the part is solidified, and the remaining molten feedstock is returned into the feedstock container for further mixing. Since the sliding platform allows the injection device to move from the feedstock container to the mold, and vice versa, an injection channel connecting the feedstock container to the gate of the mold is not required. Therefore, feedstock is not trapped between injections, and never remains idle in any component of the machine for a long time period, and thus resulting in the elimination of segregation. This new LPIM machine is therefore well adapted for the injection of low viscosity feedstock, directly resulting in a significant increase in moldability potential without producing segregation within the injection machine during the process dead time. Feedstocks were heated up to 70 or 90 °C, blended for 35 minutes under vacuum, and injected into the pre-heated spiral mold (35, 45, 50, and 60 °C) at a constant stroke of about 6 mm/s. During a typical injection, the feedstock is injected at pressures varying from 0.1 to 0.5 MPa, until there is a sudden increase in pressure (> 3 MPa), meaning that the solidification is completed or the friction with the mold walls becomes too high. Each injection condition was repeated five times.

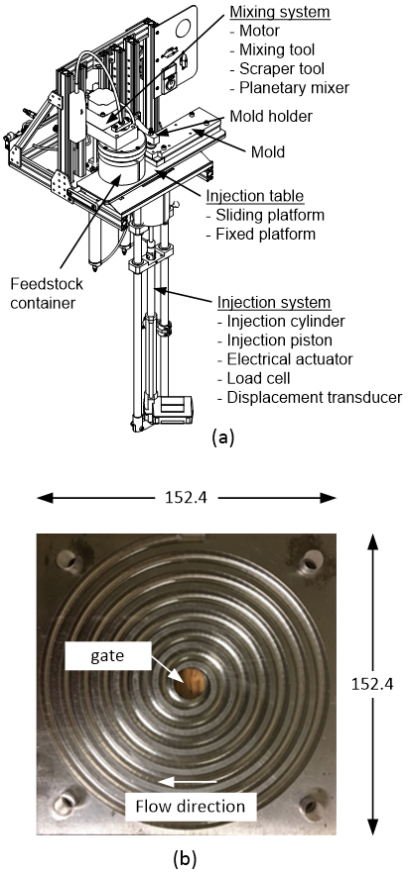


Fig. 2 (a) Injection system and (b) spiral mold (dimensions in millimeters)

## III. Results and Discussion

### *A. Transition Temperature of Feedstocks*

The DSC results for each feedstock are presented in Fig. 3. Since the feedstocks were prepared with the same proprietary

binder constituents, the two DSC thermograms are similar. These feedstocks start to melt at 39 °C, indicating the mold temperature producing a complete solidification of feedstocks (Fig. 3 (a)). In general, the latter value is used to set the mold temperature, producing a good compromise between moldability and mold sticking. The feedstocks finish melting at 66 °C, which represents the melting points of feedstocks (Figs. 3 (a) and (b)). In this context, the minimum temperature for rheological and injection tests was selected at 70 °C (i.e., an overheating of 4 °C) to ensure that all feedstocks were in the molten state.

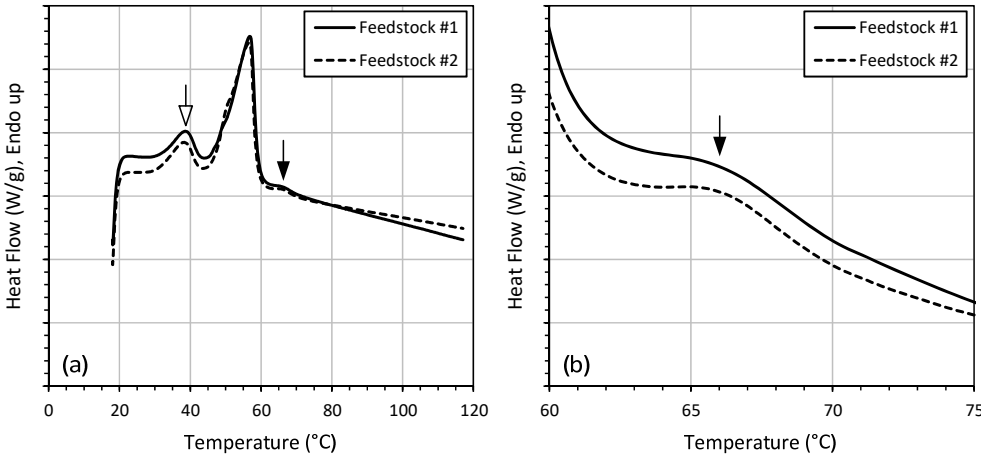


Fig. 3 (a) DSC thermograms for feedstocks; and (b) zoom within a characteristic zone showing the last DSC peaks

*B. Injection Length*

The injected length results obtained for different injection conditions are presented in Fig. 4. Typical spiral parts are represented in Fig. 4 (a) for the two feedstocks injected into a mold at 35 °C, while the injected length for different injection conditions are reported in Fig. 4 (b), where the error bars mark the standard deviations of the average injected length values (the latter are not clearly visible in Fig. 4 (b) because they are smaller than the size of the marks, as the maximum standard deviation is 16 mm). The injected lengths were calculated from the Archimedean spiral equation:

$$L = \int_0^{c*2\pi} \sqrt{(a+b\theta)^2 + b^2}\, d\theta \qquad (1)$$

where $L$ is the injected length, $a$ is the starting point of the spiral (here, $a$ = 4.7 mm in this study), $b$ is the spiral increment divided by 2π (here, $b$ = 1.516 mm in this study), $c$ is the number of turns, and $\theta$ is the angle in radian. For the two feedstocks, the injected length was influenced by the injection temperature and mold temperature. In this project, a 20 °C increase in injection temperature (e.g., from 70 to 90 °C) or a 10 °C increase in mold temperature (e.g., from 50 to 60 °C) produces a similar effect on the injected length (i.e., an increase of about 100-200 mm). Therefore, these two process parameters are useful to optimize the moldability of feedstocks. At the same injection temperature, feedstock #2 demonstrates a higher moldability potential as compared to feedstock #1 (i.e., an increase in injected length ranging from 100 to 300 mm). Since the feedstocks were prepared with the same proprietary binder constituents, this difference in moldability properties seems to be related to the powder characteristics, which will be discussed below in this paper.

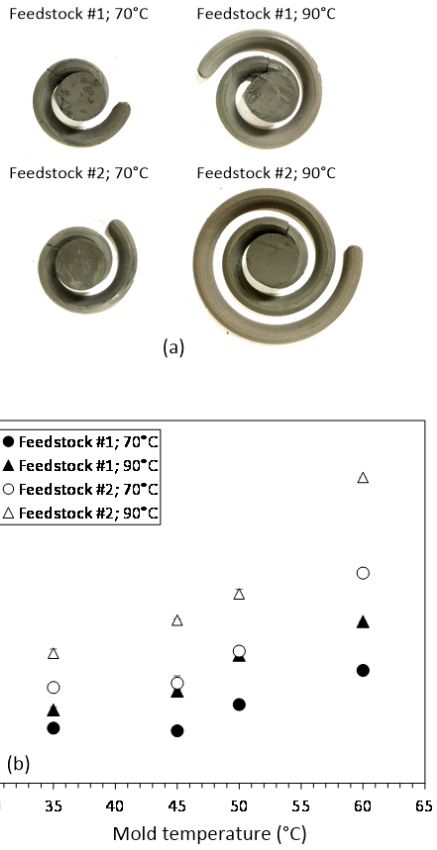


Fig. 4 (a) Typical specimens injected into the spiral mold (at $T_{mold}$ = 35 °C); (b) injected length for different injection conditions

*C. Rheological Behavior*

The viscosity profiles obtained at different temperatures are presented in Fig. 5. The viscosity of the two feedstocks decreases as the shear rate increases, up to a plateau characterized by constant viscosity values at a high shear rate. The former behavior corresponds to the shear thinning effect induced by the alignment of binder molecular chains and powder orientation with the flow. During injections, this pseudoplastic behavior is generally suitable for improving moldability of LPIM feedstocks. The second behavior corresponds to the Newtonian effect, where any increase in shear rate does not change the viscosity due to the completion of the alignment mechanism described above. For a given feedstock temperature, the pseudoplastic effect can be quantified by the following power law model widely reported in the literature:

$$\eta = K\dot{\gamma}^{n-1} \quad (2)$$

where $\eta$ is the feedstock viscosity, $\dot{\gamma}$ is the shear rate, $K$ is a constant, and $n$ is the shear rate sensitivity index. This latter parameter quantifies the degree of shear rate sensitivity during injection with a value of $n < 1$ for pseudoplastic behavior, a value of $n = 1$ for Newtonian behavior, and a value of $n > 1$ for shear thickening behavior (this undesired behavior was not observed for this feedstock). At low shear rates (i.e., before and after injection), the viscosity should be as high as possible to prevent powder-binder segregation within the injection press or the injected part. At high shear rates (i.e., during injection), the viscosity must be as low as possible to increase the moldability potential of the feedstock. Between low and high shear rates, the viscosity changes during and after the mold filling can be quantified using the value of n, which must be as small as possible. The shear rate sensitivity index ($n$) values were calculated from the $n$-1 slope of the viscosity profiles, as illustrated in Fig. 5 (a) (c.f. feedstock #1 tested at 90 °C) at shear rates ranging from 1 to 10 $s^{-1}$, and summarized in Table I, for each testing condition. In this study, the lowest shear rate sensitivity index value was associated with feedstock #1.

From a practical perspective, the rheological properties at low shear rates ($\dot{\gamma}$ = 1 $s^{-1}$) can be correlated with the feedstocks during mixing, the process dead time, or the cooldown of the injected part, while the properties calculated at moderate to high shear rates ($\dot{\gamma}$ > 100 $s^{-1}$) are useful for comparing the behavior of the feedstock during the injection stage of the process. In this respect, the moldability of a given feedstock is directly related to its viscosity. During a typical LPIM injection process, a reference viscosity $\eta_0$ associated with the shear rate inside the mold (typically $\dot{\gamma}_{ref}$ = 100 $s^{-1}$) can be extracted from viscosity curves, as illustrated in Fig. 5a (c.f. feedstock #1 tested at 70 °C) and reported in Table I. As stated above, this value should be as small as possible to improve the moldability of the feedstocks (i.e., more complex shape components at reduced pressure). From a flowability perspective, the lowest viscosity value was obtained with feedstock #2.

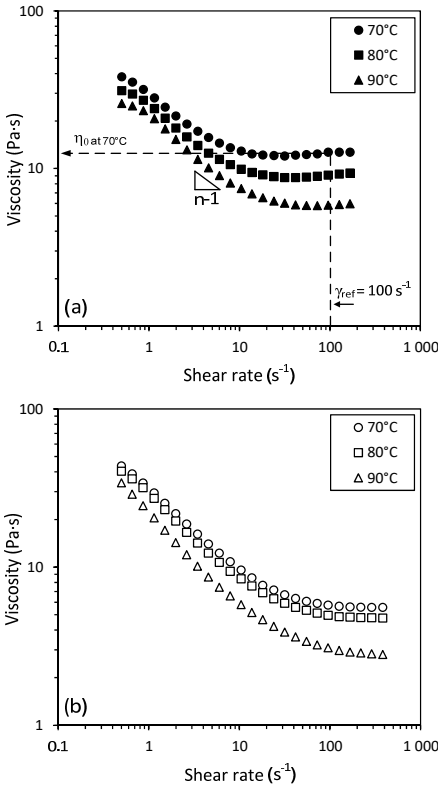


Fig. 5 Viscosity profiles for feedstocks tested at 70, 80, and 90 °C (a) feedstock #1; (b) feedstock #2

The viscosity profiles presented in Fig. 5 also indicate that the viscosity values of Co-Cr-based feedstocks are relatively dependent on the feedstock temperature. Indeed, the viscosity of all feedstocks decreases as the temperature increases, indicating that the binder chain molecules move more easily at higher temperatures. This influence of the temperature on the rheological behavior can be described by Arrhenius equation:

$$\eta = \eta_{To} \exp\left(\frac{E}{RT}\right) \quad (3)$$

where $\eta$ is the viscosity, $\eta_{T0}$ is the viscosity at a reference temperature, $E$ is the activation energy for viscous flow, $R$ is the gas constant, and $T$ is the temperature. The value of the activation energy is used to quantify the degree of the temperature sensitivity to the feedstock viscosity. In fact, the value of $E$ quantifies the tendency of feedstock to exhibit sudden viscosity changes due to small temperature gradients during injection (i.e., between the hot and cold zones in the injection press or in the mold). This value should be as low as possible to minimize changes in feedstock viscosity during the process. At the reference shear rate (i.e., $\dot{\gamma}_{ref}$ = 100 $s^{-1}$), the

values for the natural logarithm of the viscosity $\eta_0$ were plotted against $1/T$ in Fig. 6 to calculate the values of $E$ from the slope of each graph, which were summarized in Table I. In this study, both feedstocks exhibit similar temperature sensitivity.

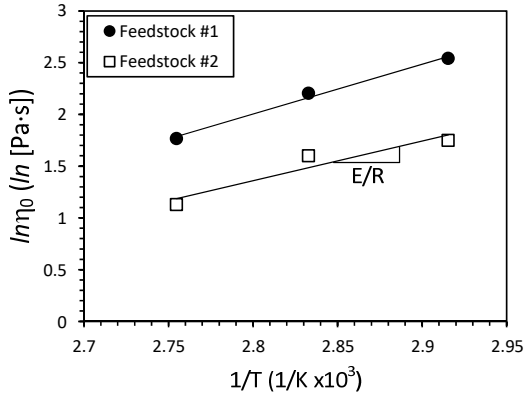


Fig. 6 Dependence of viscosity on temperature for calculation of the activation energy for viscous flow

TABLE I
RHEOLOGICAL PROPERTIES OF FEEDSTOCKS

| Feedstock # | T feedstock (°C) | $\eta_0$ (Pa·s) | $n$ | $E$ (kJ/mol) |
|---|---|---|---|---|
| 1 | 70 | 12.7 | 0.65 | |
| 1 | 80 | 9.1 | 0.60 | 40.0 |
| 1 | 90 | 5.9 | 0.53 | |
| 2 | 70 | 5.7 | 0.53 | |
| 2 | 80 | 5.0 | 0.52 | 31.9 |
| 2 | 90 | 3.1 | 0.48 | |

Rheological properties such as the reference viscosity ($\eta_0$), the shear rate sensitivity index ($n$), and the activation energy for viscous flow ($E$) can be combined together into the Weir's model [12] to assess the moldability index ($\alpha_{STV}$) of feedstocks.

$$\alpha_{STV} = \frac{10^7}{\eta_o} \frac{|n-1|}{E/R} \quad (4)$$

Initially developed to study the molding performance of plastic during injection, this original model has been used successfully by many research teams to optimize feedstock formulations [13]-[19]. The strength of the model lies in its quantification of the moldability of a feedstock without the need to perform long and expensive injections. From (4), the best feedstock candidate corresponds to the highest value of $\alpha_{STV}$, which is obtained for the lowest value of $\eta_0$, $n$, and $E$, concurrently. The moldability index values were validated with the injected length obtained with the real scale injections (Fig. 7). Feedstock #2 exhibited the highest $\alpha_{STV}$ value, indicating a good compromise of the rheological characteristics, also leading to better molding properties as compared to feedstock #1. Rheological properties, such as the reference viscosities, the shear rate sensitivity index, and the activation energy calculated with feedstock #2 (summarized in Table I) are all beneficial, as compared to that obtained with feedstock #1. Therefore, the moldability index value for feedstock #2 is higher than that calculated for feedstock #1.

For these two Co-Cr-based feedstocks, the trend of the moldability index values calculated with the Weir's model is in good agreement with the real scale injection results. As shown in Fig. 7, the model was successfully used to identify feedstock #2 as the mixture producing the best moldability properties. These results confirm that this simple model (i.e., the one that uses indirect measurement to predict the moldability properties of feedstocks) can be used during the development of new feedstock formulations, or in the quality control of feedstock in production to confirm the molding capability of LPIM feedstocks or to identify the future injection problem, as demonstrated with the powder batches used in this project. Indeed, the feedstocks were formulated with two different powder batches delivered to production specifications. In this respect, a priori, the visualization of the dry powders (Fig. 1) confirms similar powder size and powder distribution. However, the surfaces of powder #1 seem to be more textured (i.e., unlike the smooth surface) than those of feedstock #2. In addition, powder lot #1 seems to be characterized by more small satellite particles (i.e., small particles < 1 µm stuck on large particles), as compared to powder lot #2. These differences in initial powder lots probably represent the root cause of the significant difference in rheological behavior and injection properties reported in Fig. 7.

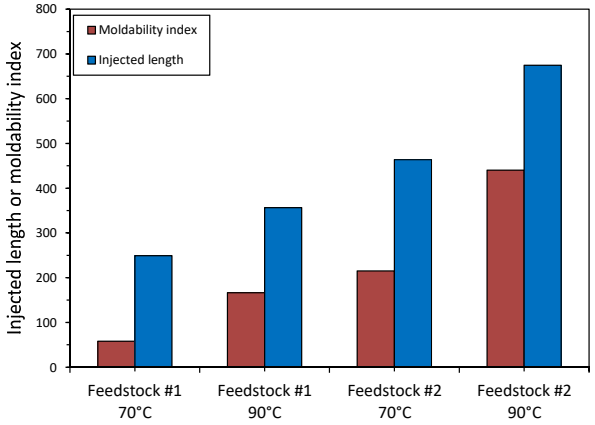


Fig. 7 Comparison of the injected length ($T_{mold}$ = 60 °C) and moldability index for viscosity values obtained at a reference shear rate $\dot{\gamma}_{ref}$ = 100 $s^{-1}$

## IV. CONCLUSIONS

The moldability of two proprietary Co-Cr LPIM feedstocks was investigated. The moldability indexes calculated from the rheological properties of feedstocks were compared to the real scale injection results, leading to the following conclusions:

- Since the feedstocks were formulated with the same binder constituents, the first DSC peak (indicating an appropriate mold temperature value) and the last DSC

peak (representing the melting point of the feedstock) are similar.

- The injection length was significantly influenced by the mold temperature, the feedstock temperature, and the powder characteristics.
- The viscosity of all feedstocks decreased with the shear rate (i.e., the shear thinning behavior generally required for LPIM feedstocks) before stabilizing at a constant value at high shear rates. The viscosity values were also affected by the feedstock temperature and the powder characteristics.
- In this project, the trend of the moldability index values calculated with the Weir's model was in good agreement with real scale injection results. The model was successfully used to predict the Co-Cr feedstock demonstrating the best moldability properties during the injection step of the process. This model can thus be used during the development of new feedstock formulations or for quality control of feedstock in production, in order to confirm the molding capability of Co-Cr feedstocks.

## ACKNOWLEDGMENT

This work was carried out with the financial support of the Natural Sciences and Engineering Research Council of Canada.

## REFERENCES

[1] M. Aslam, F. Ahmad, P. S. M. B. M. Yusoff, K. Altaf, M. A. Omar, H. P. S. Abdul Khalil, M. R. Raza, Investigation of Rheological Behavior of Low Pressure Injection Molded Stainless Steel Feedstocks, Advances in Materials Science and Engineering, 2016 (2016).

[2] G. Wen, P. Cao, B. Gabbitas, D. Zhang, N. Edmonds, Development and design of binder systems for titanium metal injection molding: An overview, Metall. Mater. Trans. A, 44 (2013) 1530-1547.

[3] R. Ibrahim, M. Azmirruddin, M. Jabir, N. Johari, M. Muhamad, A.R.A. Talib, Injection Molding of Inconel 718 Parts for Aerospace Application Using Novel Binder System Based on Palm Oil Derivatives, International Journal of Mechanical, Aerospace, Industrial, Mechatronic and Manufacturing Engineering, 6 (2012) 2112-2116.

[4] M. E. Sotomayor, A. Cervera, A. Várez, B. Levenfeld, Duplex Stainless Steel Self-ligating Orthodontic Brackets by Micro-powder Injection Moulding, International Journal of Engineering Research & Science, 2 (2016) 184-193.

[5] B. Hausnerova, Powder injection moulding-An alternative processing method for automotive items, InTech, 2011.

[6] D. Heaney, Woodhead Publishing, 2012, pp. 604.

[7] J. González-Gutiérrez, G.B. Stringari, I. Emri, Powder Injection Molding of Metal and Ceramic Parts, InTech, 2012.

[8] M. R. Harun, N. Muhamad, A. B. Sulong, N. H. M. Nor, M. H. I. Ibrahim, Rheological investigation of ZK60 magnesium alloy feedstock for metal injection moulding using palm stearin based binder system, Applied Mechanics and Materials, 44-47 (2011) 4126-4130.

[9] N. H. M. Nor, M. H. Ismail, N. A. Abu Kasim, N. Muhamad, M. A. Taib, Characterization and rheological studies on ready-made feedstock of stainless steel 316L in metal injection molding (MIM) process, Applied Mechanics and Materials, 465-466 (2014) 709-714.

[10] V. Demers, S. Turenne, O. Scalzo, Impact of binders on viscosity of low-pressure powder injection molded Inconel 718 superalloy, Journal of Materials Science, 50 (2015) 2893-2902.

[11] J. Hidalgo, A. Jimnez-Morales, T. Barriere, J.C. Gelin, J. M. Torralba, Capillary rheology studies of INVAR 36 feedstocks for powder injection moulding, Powder Technol., 273 (2015) 1-7.

[12] F. E. Weir, M. E. Doyle, D. G. Norton, Moldability of plastics based on melt rheology, SPE Transactions, 3 (1963) 32-41.

[13] P. Seong-Jin, W. Yunxin, D. Heaney, Z. Xin, G. Guosheng, R. German, Rheological and thermal debinding behaviors in titanium powder injection molding, Metallurgical and Materials Transactions A (Physical Metallurgy and Materials Science), 40 (2009) 215-222.

[14] C. Joon-Phil, L. Hyun-Gon, L. Won-Sik, L. Jai-Sung, Investigation of the rheological behavior of 316L stainless steel micro-nano powder feedstock for micro powder injection molding, Powder Technol., 261 (2014) 201-209.

[15] H. Abdoos, H. Khorsand, A. A. Yousefi, Torque rheometry and rheological analysis of powder-polymer mixture for aluminum powder injection molding, Iranian Polymer Journal, 23 (2014) 745-755.

[16] M. H. I. Ibrahim, N. Muhamad, A.B. Sulong, Rheological investigation of water atomised stainless steel powder for micro metal injection molding, International Journal of Mechanical and Materials Engineering, 4 (2009) 1-8.

[17] A. Ghanbari, M. Alizadeh, E. Ghasemi, R. Y. Rad, S. Ghaffari, Preparation of optimal feedstock for low-pressure injection molding of Al/SiC nanocomposite, Science and Engineering of Composite Materials, 22 (2015) 549-554.

[18] N. N. Ismail, K. R. Jamaludin, N. Ahmad, Glycerol As Plasticizer For Waste Polystyrene Based Metal Injection Molding (MIM) Binder, Advanced Materials Research, 845 (2014) 837-840.

[19] V. Demers, M. M. Elmajdoubi, P. Bocher, 2017 World Congress on Powder Metallurgy and Particulate Materials, PowderMet 2017, June 13, 2017 - June 16, 2017, Metal Powder Industries Federation, Las Vegas, NV, United States, 2017, pp. 401-414.

[20] G. C. Babis, A. F. Mavrogenis, Cobalt–Chrome Porous-Coated Implant-Bone Interface in Total Joint Arthroplasty, in: T. Karachalios (Ed.) Bone-Implant Interface in Orthopedic Surgery: Basic Science to Clinical Applications, Springer London, London, 2014, pp. 55-65.

[21] Z. Y. Liu, N. H. Loh, S. B. Tor, K. A. Khor, Characterization of powder injection molding feedstock, Mater. Charact., 49 (2003) 313-320.

[22] S. G. Lamarre, V. Demers, J.-F. Chatelain, Low-pressure powder injection molding using an innovative injection press concept, The International Journal of Advanced Manufacturing Technology, (2017) 1-11.